Artificial muscle-like function from hierarchical supramolecular assembly of photoresponsive molecular motors

Chen, Jiawen; Leung, Franco King-Chi; Stuart, Marc C. A.; Kajitani, Takashi; Fukushima, Takanori; van der Giessen, Erik; Feringa, Ben L.

Published in:
Nature Chemistry

DOI:
10.1038/nchem.2887

ARTICLES
PUBLISHED ONLINE: 4 DECEMBER 2017 | DOI: 10.1038/NCHEM.2887
nature chemistry

Artificial muscle-like function from hierarchical supramolecular assembly of photoresponsive molecular motors

Jiawen Chen[1†], Franco King-Chi Leung[1,2†], Marc C. A. Stuart[1], Takashi Kajitani[2,3], Takanori Fukushima[2], Erik van der Giessen[4] and Ben L. Feringa[1*]

A striking feature of living systems is their ability to produce motility by amplification of collective molecular motion from the nanoscale up to macroscopic dimensions. Some of nature's protein motors, such as myosin in muscle tissue, consist of a hierarchical supramolecular assembly of very large proteins, in which mechanical stress induces a coordinated movement. However, artificial molecular muscles have often relied on covalent polymer-based actuators. Here, we describe the macroscopic contractile muscle-like motion of a supramolecular system (comprising 95% water) formed by the hierarchical self-assembly of a photoresponsive amphiphilic molecular motor. The molecular motor first assembles into nanofibres, which further assemble into aligned bundles that make up centimetre-long strings. Irradiation induces rotary motion of the molecular motors, and propagation and accumulation of this motion lead to contraction of the fibres towards the light source. This system supports large-amplitude motion, fast response, precise control over shape, as well as weight-lifting experiments in water and air.

Movement is one of the vital features of living systems, and the construction of soft actuators such as artificial muscle-like materials, which can change shape and perform mechanical functions in response to energy input, offer fascinating prospects[1–5]. Taking inspiration from nature for the development of synthetic systems that are stimuli-responsive and capable of converting molecular motion into macroscopic movement, it is of paramount importance to precisely control molecular organization and cooperativity to allow amplification of motion by many orders of magnitude. One approach is based on stimuli-responsive crystals, and for this, high positional molecular order is key to inducing deformation of the crystals[6–9]. Another important approach is to introduce molecular machines, such as switches[10], shuttles[11] and motors[12], into covalent macromolecular materials to produce, for example, responsive (conjugated) polymers[13], polymeric gels[14–17] and polymer liquid crystals[18–22]. Here, in contrast to these polymer networks or crystal reshaping, we report a muscle-like system based on hierarchical supramolecular organization of small molecules. This system addresses the fundamental question of whether cooperative non-covalent interactions in water can allow amplification of a photo-induced response along many length scales in order to sustain a macroscopic mechanical motion.

Following pioneering work by Sauvage on molecular muscles[23,24] and attempts to generate controlled motion via hierarchical organized non-covalent supramolecular assemblies[25–27], recent efforts toward soft actuators have focused on rotaxanes[28] and host–guest complexes[29]. Although important steps towards the amplification of molecular motion at higher length scales have been made[30,31], a remaining challenge is to use small-molecule self-assembly to amplify molecular motion all the way to macroscopic movement in water[32,33], as seen in natural systems. The fragile and highly dynamic nature of self-assembly at the molecular level has precluded, until now, the achievement of sufficient control over the self-assembly and cooperativity of stimuli-responsive molecules to demonstrate macroscopic muscle-like responses.

Result and discussion

Design of supramolecular muscle. We selected the following key features: (1) a non-polymeric small-molecule-based system, (2) an intrinsically responsive molecule that allows hierarchical self-organization, (3) the use of a non-invasive light stimulus to induce motion with high spatial-temporal precision, (4) a supramolecular muscle-like system that should operate both in water and air, and (5) amplification of motion from the molecular level over various length scales to a macroscopic contractile movement. In our design, amphiphilic molecular motor **1** is attached to a dodecyl chain to form the upper half and to two carboxyl groups to enhance water solubility, connected via two alkyl-linkers, to form the lower half, endowing the resultant nanofibre-assembled structure with the flexibility to facilitate microphase separation and molecular reordering in an aqueous medium (Fig. 1a). To avoid complicated processes (such as crystallization) and to build up the soft responsive material featuring hierarchical supramolecular organization of motor **1**, electrostatic screening using calcium ions and shear flow was used to form a string of unidirectional alignment nanofibre bundles[34]. We envisioned that upon exposure of this highly organized hierarchical supramolecular structure to a light source, the generated rotary motion would be propagated and amplified to provide photoactuation of macroscopic motion.

It is expected that when a stable motor isomer (**Stable-1**) with the methyl group at the stereogenic centre in a pseudo-axial

[1]Stratingh Institute for Chemistry, University of Groningen, Nijenborgh 4, 9747AG Groningen, The Netherlands. [2]Laboratory for Chemistry and Life Science, Institute of Innovative Research, Tokyo Institute of Technology, 4259 Nagatsuta, Midori-ku, Yokohama 226-8503, Japan. [3]RIKEN SPring-8 Center, 1-1-1 Kouto, Sayo, Hyogo 679-5148, Japan. [4]Zernike Institute for Advanced Materials, University of Groningen, 9747AG Groningen, The Netherlands. †These authors contributed equally to this work. *e-mail: b.l.feringa@rug.nl

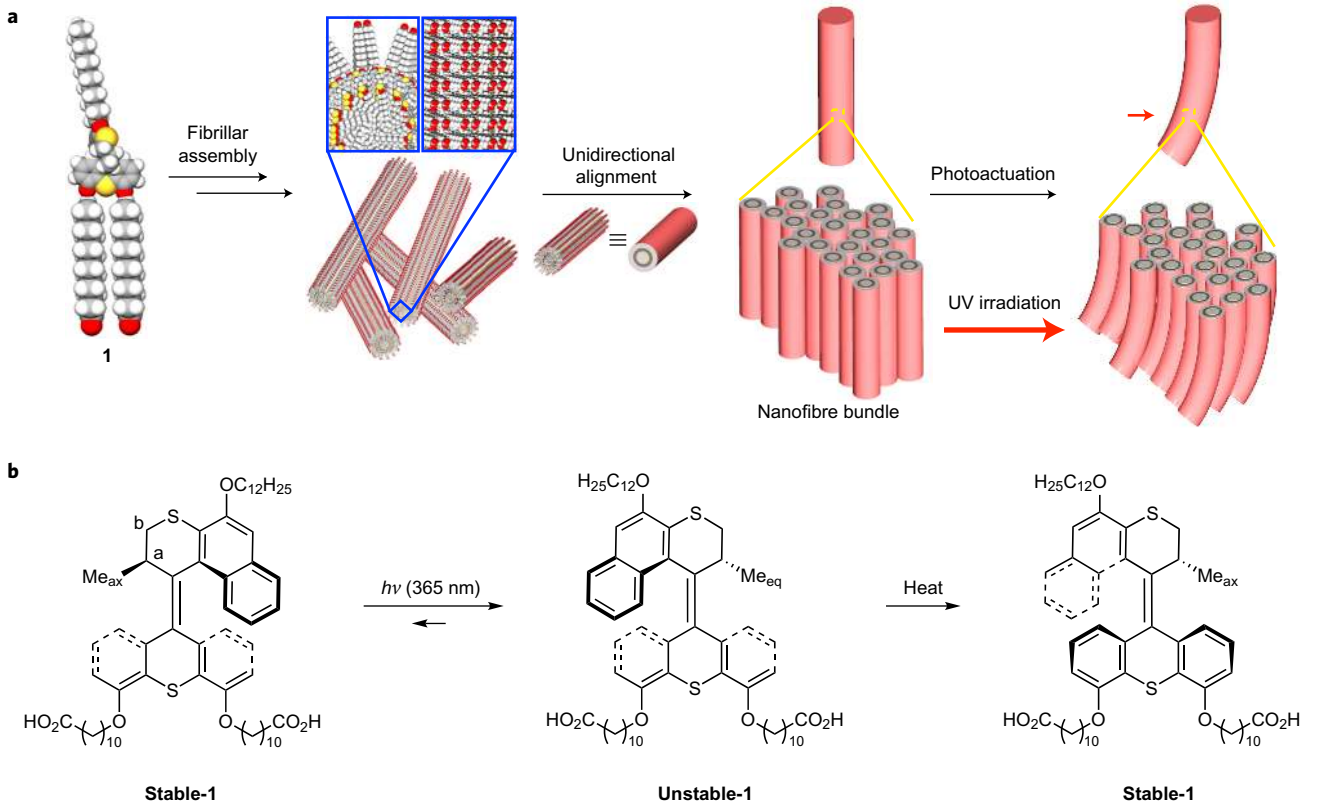

Figure 1 | Representative scheme for the preparation and photoactuation of a macroscopic string. a, Structure of photoresponsive rotary motor **1** and its self-assembly into nanofibres. The nanofibre-containing solution is manually drawn from a pipette into a $CaCl_2$ solution to achieve unidirectional alignment in bundles, generating a string that is able to bend upon exposure to UV irradiation (represented by red arrows). Colour code for space-filling model: grey, C; red, O; yellow, S; white, H. **b**, Photochemical and thermal helix inversion steps of motor **1**. A single enantiomer is shown; the two **Stable-1** isomers shown are identical but viewed from different angles.

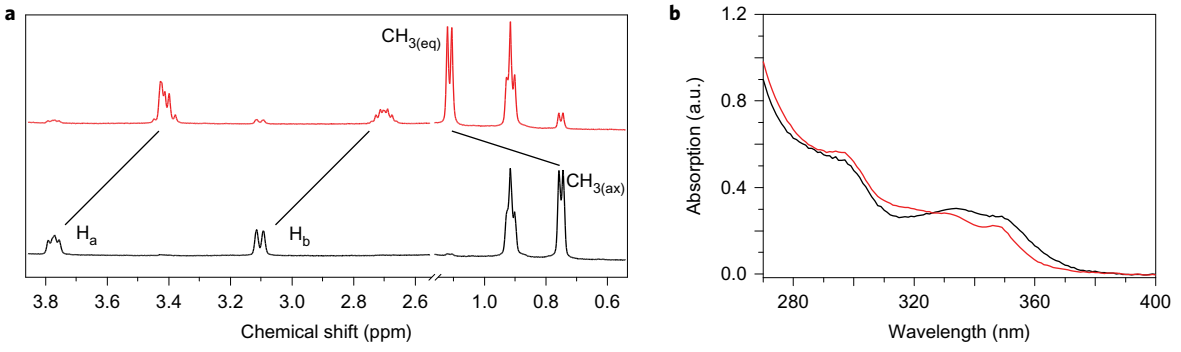

Figure 2 | Light-responsive motion of molecular motor 1. a, Selected parts of ^{1}H NMR spectra (CD_2Cl_2, 25 °C, 500 MHz) of **Stable-1** (black) and a photostationary state mixture (red) containing 90% **Unstable-1** after irradiation. **b**, UV–vis absorption spectra of a self-assembled nanofibres solution of **1** in water (2 mg ml^{-1}) before (black) and after (red) irradiation.

orientation is irradiated with UV light (λ = 365 nm), photochemical isomerization around the central alkene bond takes place (Fig. 1b). This photochemical step results in an unstable isomer (**Unstable-1**), in which the methyl moiety at the stereogenic centre is forced to adopt an energetically unfavoured pseudo-equatorial orientation. To release steric strain, the unstable isomer undergoes an irreversible thermal helix inversion step, generating the stable isomer (**Stable-1**) in which the stereogenic methyl substituent again adopts a more favoured pseudo-axial orientation (Fig. 1b), completing the rotary cycle.

The synthesis and characterization of motor **1** are detailed in Supplementary Section 1. Due to its amphiphilic nature, compound **1** is able to undergo self-assembly in water to form a solution containing nanofibres. This solution is then drawn manually from a pipette into aqueous Ca^{2+} solution to form strings centimetres in length (Fig. 1a). The obtained macroscopic string shows long-range unidirectional alignment of the nanofibres inside. Phototriggered actuation of the string can be achieved both in aqueous solution and in air.

Photoisomerization and self-assembly. The photochemical and thermal isomerization steps of **1** were examined by NMR and UV–vis spectroscopy. Figure 2a shows the aliphatic region of the ^{1}H NMR spectrum (black) of **Stable-1** in CD_2Cl_2 solution.

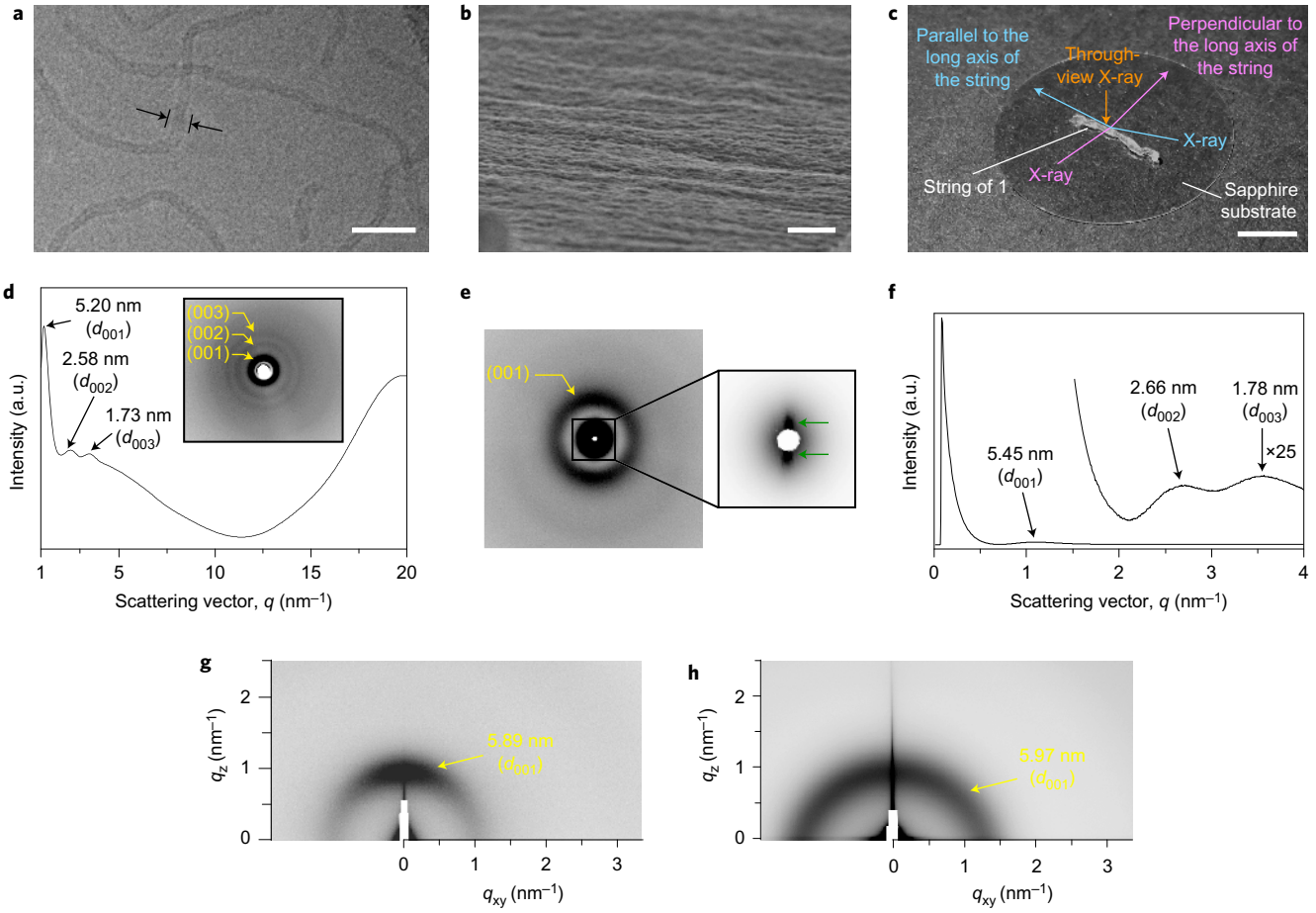

Figure 3 | Electronic microscopies and X-ray analysis of a macroscopic string prepared from 1 on a sapphire substrate. a, Cryo-TEM image of nanofibres composed of **1** (0.5 wt%). Black arrows indicate the width of the nanofibres. Scale bar, 25 nm. **b**, SEM image of a string (5 wt%). Scale bar, 5 μm. **c,** Schematic illustration of the experimental setup for 2D GI-SAXS, through-view WAXD and SAXS. Scale bar, 0.5 cm. **d**, 1D WAXD pattern and 2D image (inset) at 25 °C. Scattering vector $q = 2\pi/d$. The diffraction peaks corresponding to *d* spacings of 5.20, 2.58 and 1.73 nm are indexed as diffractions from the (001), (002) and (003) planes, respectively, of a string consisting of unidirectionally aligned nanofibres. **e**, 2D SAXS images (inset: enlarged 2D image for $q = 0.1$–0.45 nm^{-1}) at 25 °C. Yellow arrows in **d** and **e** indicate positions of diffraction planes. Green arrows (inset, **e**) indicate positions of a pair of spot-like scatterings arising from the aligned nanofibre bundles. **f**, 1D SAXS pattern at 25 °C showing diffraction corresponding to *d* spacings of 5.45, 2.66 and 1.78 nm, arising from the (001), (002) and (003) planes, respectively, in the direction perpendicular to the long axis of the string. **g**,**h**, 2D GI-SAXS images observed at 25 °C upon exposure to an X-ray beam from the directions perpendicular (**g**) and parallel (**h**) to the long axis of the string. Values in parentheses indicate Miller indices of the corresponding planes. The diffraction spot in the perpendicular direction of the string and the isotropic ring in the parallel direction also support alignment of the nanofibres.

Following UV irradiation ($\lambda = 365$ nm), three distinct changes were observed (Fig. 2a, red), indicating conversion from **Stable-1** to **Unstable-1**. The doublet at $\delta = 0.77$ ppm, which is characteristic of the methyl group adjacent to the stereogenic centre, was observed to shift downfield to $\delta = 1.13$ ppm (Fig. 2a, red). This can be attributed to the increased deshielding experienced by the pseudo-equatorial methyl group, which is positioned closer to the lower-half arene moiety in **Unstable-1** compared to the stable isomer, in accordance with the conformational change of the methyl group from a pseudo-axial to a pseudo-equatorial orientation. In addition, signals of H_a and H_b from the aliphatic protons in the upper half shift upfield from $\delta = 3.79$ ppm (multiplet) and $\delta = 3.12$ ppm (double doublet) in **Stable-1** to $\delta = 3.41$ ppm (multiplet) and $\delta = 2.71$ ppm (multiplet) in **Unstable-1** (Fig. 2a, red). It manifests the difference in conformation of the six-membered ring of **Stable-1** and **Unstable-1**.

Notably, extended irradiation resulted in a photostationary state with an **Unstable-1**/**Stable-1** ratio of 90:10. Thermal helix inversion from **Unstable-1** to **Stable-1** can be induced by keeping the sample at 50 °C overnight, which results in recovery of the original spectrum. The rate constants of the thermal process were studied by means of Eyring analysis (Supplementary Fig. 1), and a Gibbs free energy of activation ($\Delta^{\ddagger}G^0$) of 104.1 kJ mol^{-1} was obtained, which corresponds to a half-life ($t_{1/2}$) of 128 h at 20 °C and 2.7 h at 50 °C. In addition, the photochemical and thermal helix inversion steps were confirmed by UV–vis absorption spectroscopy. Upon irradiation, the spectrum shows an increase in the absorption around 310 nm with a concomitant decrease of the absorption band from 340 nm to 370 nm (Supplementary Fig. 2a). An isosbestic point at 327 nm over the course of the irradiation suggests a selective isomerization process. These spectral changes are in accordance with those observed for the related unfunctionalized motor[35], indicating the formation of **Unstable-1**. After warming of the sample, the original spectrum was regenerated, confirming thermal isomerization to **Stable-1**.

The self-assembly of motor **1** in water was investigated by cryogenic transmission electron microscopy (cryo-TEM). In the presence of 2 equiv. of NaOH, motor **1** forms nanofibres with a high aspect ratio under aqueous conditions (Fig. 3a). These nanofibres are several micrometres in length and have a diameter of

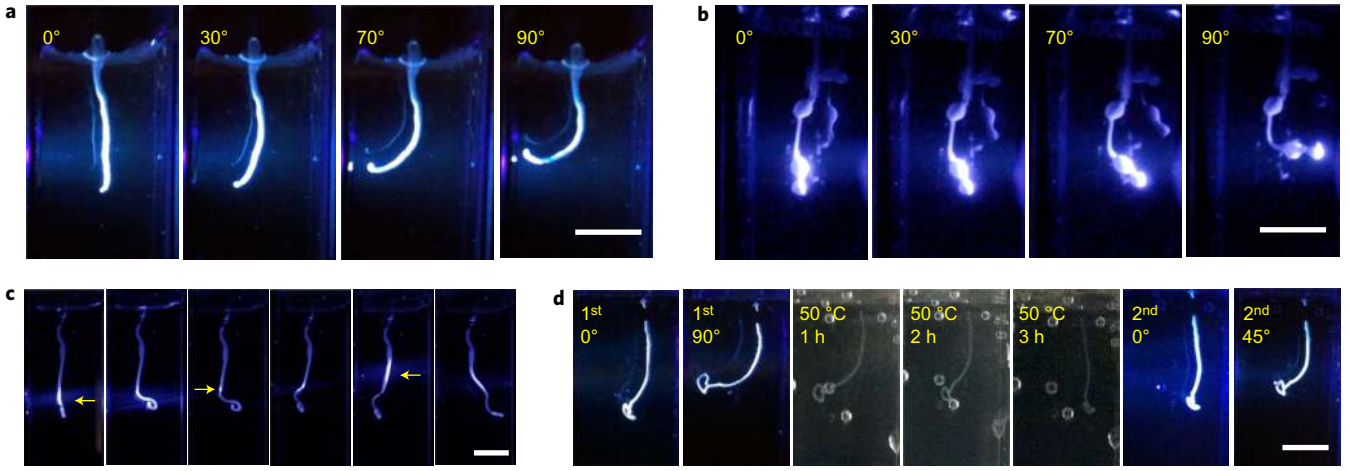

Figure 4 | Photoactuation and thermal reversible process of the molecular motor-based string in aqueous solution. a, Snapshots of a supramolecular string in water after irradiation from the left. The string bends towards the UV light from 0° to 90° within 60 s. **b**, Snapshots of a motor string that contains a bulky ball-shaped end. The ball-shaped part is able to bend towards the UV light (from the right) to 90° within 1 min. **c**, Snapshots of a motor string after sequential point irradiation from alternate directions, resulting in a zigzag conformation. Irradiation is indicated by yellow arrows. **d**, Photo- and thermal actuation of the motor string. The first irradiation results in bending of the string to the left around 90°. After maintaining the solution at 50 °C for 3 h, the string returns to its original conformation. A second irradiation causes the string to bend to the left again. Irradiation is provided by a light-emitting diode ($\lambda = 365$ nm). Scale bars for all panels, 0.5 cm.

~5–6 nm. UV–vis absorption spectral studies showed that the photochemical and thermal isomerization processes of motor **1** in the self-assembled structures in water are fully preserved (Fig. 2c and Supplementary Fig. 2a). When the motor-based nanofibre solution was manually drawn into an aqueous solution of $CaCl_2$ (150 mM), a noodle-like string with arbitrary length was formed (Supplementary Movie 1). Notably, a minimum 5 wt% of motor is needed for preparation of the string. In polarized optical microscopy (POM), the resulting string exhibits uniform birefringence in the direction of its long axis (Supplementary Fig. 3). Scanning electronic microscopy (SEM) of the string shows arrays of unidirectionally aligned nanofibre bundles (Fig. 3b). The through-view wide-angle X-ray diffraction (WAXD) of a string prepared on a sapphire substrate (Fig. 3c) displays diffraction peaks with d spacings of 5.20, 2.58 and 1.73 nm, which are indexed as diffractions from the (001), (002) and (003) planes, respectively, of a lamellar structure (Fig. 3d). The layer spacing of the lamellar structure ($c = 5.19$ nm) is comparable to the average diameter (~6 nm) of the nanofibres of **1** observed in cryo-TEM (Fig. 3a). Based on the electron microscopic and WAXD data, the string should consist of unidirectionally aligned nanofibre bundles of **1**. To investigate the orientational order of the bundled nanofibres in the macroscopic string, we carried out through-view small-angle X-ray scattering (SAXS) and grazing-incident SAXS (GI-SAXS) experiments. In the two-dimensional (2D) SAXS image (Fig. 3e), a pair of spot-like scatterings is observed in a smaller-angle region ($q = 0.1$–0.45 nm^{-1}; Fig. 3e, inset)[34], which is due to scatterings from the unidirectionally aligned nanofibre bundles. Importantly, the diffraction arcs with d spacings of 5.45, 2.66 and 1.78 nm (Fig. 3f), arising from diffractions from the (001), (002) and (003) planes, respectively, appear in the meridional direction (Fig. 3e), that is, the direction perpendicular to the long axis of the string. GI-SAXS data (Fig. 3g,h) also indicate that the nanofibre bundles align unidirectionally along the long axis of the string. When the incident X-ray beam was perpendicular to the long axis of the string, a diffraction spot (d spacing = 5.89 nm) from the (001) plane appeared in the meridional direction (Fig. 3g). The diffraction was observed as an isotropic ring when the incident X-ray beam was parallel to the long axis of the string (Fig. 3h).

Photoactuation in water. A string formed by self-assembly of motor **1** was studied in a cuvette containing an aqueous solution of $CaCl_2$ (150 mM). Upon photoirradiation ($\lambda = 365$ nm), the string of motor **1** bent towards the light, representing the first direct observation of macroscopic motion of a hierarchical supramolecular non-covalent system based on a photoresponsive molecular motor (Fig. 4a and Supplementary Movie 2). The string bent from an initial angle of 0° to a saturated flexion angle of 90° within 60 s, which is proof of large-amplitude actuation and fast actuation ($1.5 \pm 0.02°$ s^{-1}). Noticeably, the string of small-molecule motor **1**, containing 95% water in the supramolecular material, provides a remarkably fast response compared to a photoresponsive polymeric hydrogel, which produces a smaller actuation at lower speed (0.14° min^{-1})[14]. A string featuring a bulky ball-shaped end, that is, 10 times larger in size than the rest of the string, showed a bending motion with a saturated flexion angle (90°) within 60 s, which is comparable to that of the normal string (Fig. 4b and Supplementary Movie 3). Subsequently, a string of motor **1** (1.2 cm in length) was irradiated alternately from either right or left sides at various positions of the string in a sequential manner, and the resulting string showed a zigzag conformation, indicating that localized motions of the current system were achieved (Fig. 4c and Supplementary Movie 4). A string that had bent towards the light source with a flexion angle of 90° after photoirradiation was then heated at 50 °C in the dark (Fig. 4d). The string returned to its original conformation within 3 h, which is in accordance with the half-life of motor **1** ($t_{1/2} = 2.7$ h at 50 °C, Supplementary Fig. 1). Following a second photoirradiation, the same string was found to bend to a flexion angle of ~45°. The results indicate successful photoactuation and a thermally reversible process for the string. Retardation of the system after the first reversible cycle is attributed to instability of the supramolecular string at the relatively high temperature used for the thermal helix inversion process.

Photoactuation in air. A string prepared by the above-mentioned method was pulled out of the aqueous $CaCl_2$ solution and suspended in air (Fig. 5a). Upon photoirradiation ($\lambda = 365$ nm), the string was able to bend towards the light source to a saturated flexion angle (90°) within 50 s (Fig. 5a and Supplementary Movie 5),

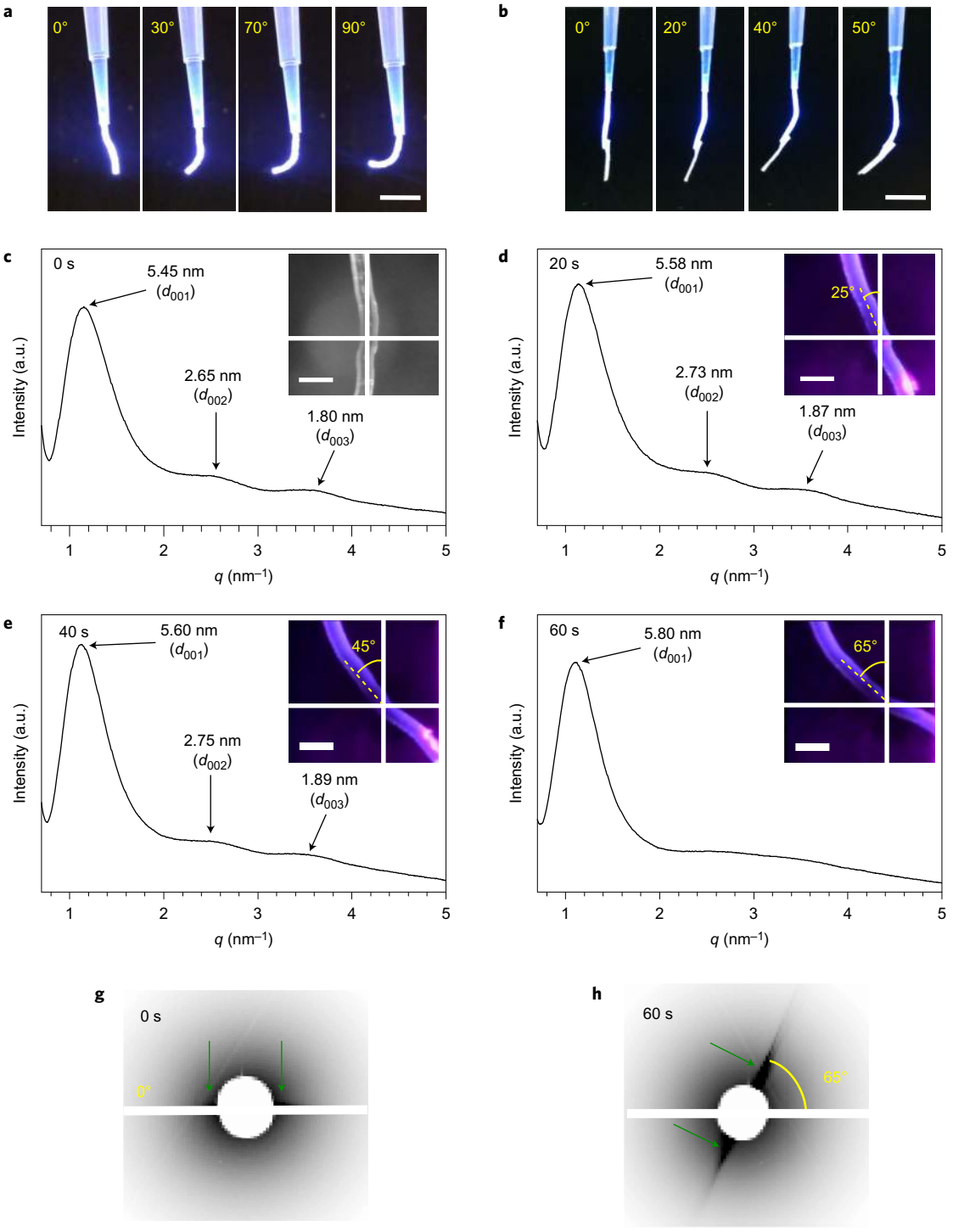

Figure 5 | Photoactuation in air and *in situ* SAXS of a macroscopic string prepared from 1. a,**b**, Photographs of the photoactuation upon irradiation with UV light for ~50 s in air without weight (**a**) and with 0.4 mg paper as weight (**b**). Scale bars, 0.5 cm. **c**–**f**, 1D SAXS patterns and photographs (inset scale bars, 500 μm) of a string suspended in air after UV irradiation at 25 °C for 0 s (**c**), 20 s (**d**), 40 s (**e**) and 60 s (**f**). Intersections of the two white lines in the photographs represent the centre of the X-ray beam. Values in parentheses in the 1D SAXS patterns indicate Miller indices. **g**,**h**, 2D SAXS images (q = 0.1–0.45 nm^{-1}) after irradiation for 0 s (**g**) and 60 s (**h**). Green arrows indicate positions of the pair of spots arising from the aligned nanofibre bundles (in the same manner as Fig. 3e) and the angle shows the bending of the string.

which corresponds to a speed of 1.8 ± 0.07° s^{-1}. To demonstrate the intrinsic potential of this photoactuation process, a lifting experiment was performed in air (Fig. 5b and Supplementary Movie 6). As shown in Fig. 5b, a 0.4 mg piece of paper was adhered to the end of a string. Following photoirradiation, the string was capable of bending by 45° towards the light source, indicating that the string has sufficient actuation power to lift weight. The mechanical work that the system performed during this process was calculated to be 0.05 μJ (Supplementary Fig. 12).

To investigate the structural changes during photoactuation, we carried out *in situ* SAXS measurements (Fig. 5c–h and Supplementary Movie 7). We suspended a string from a sample

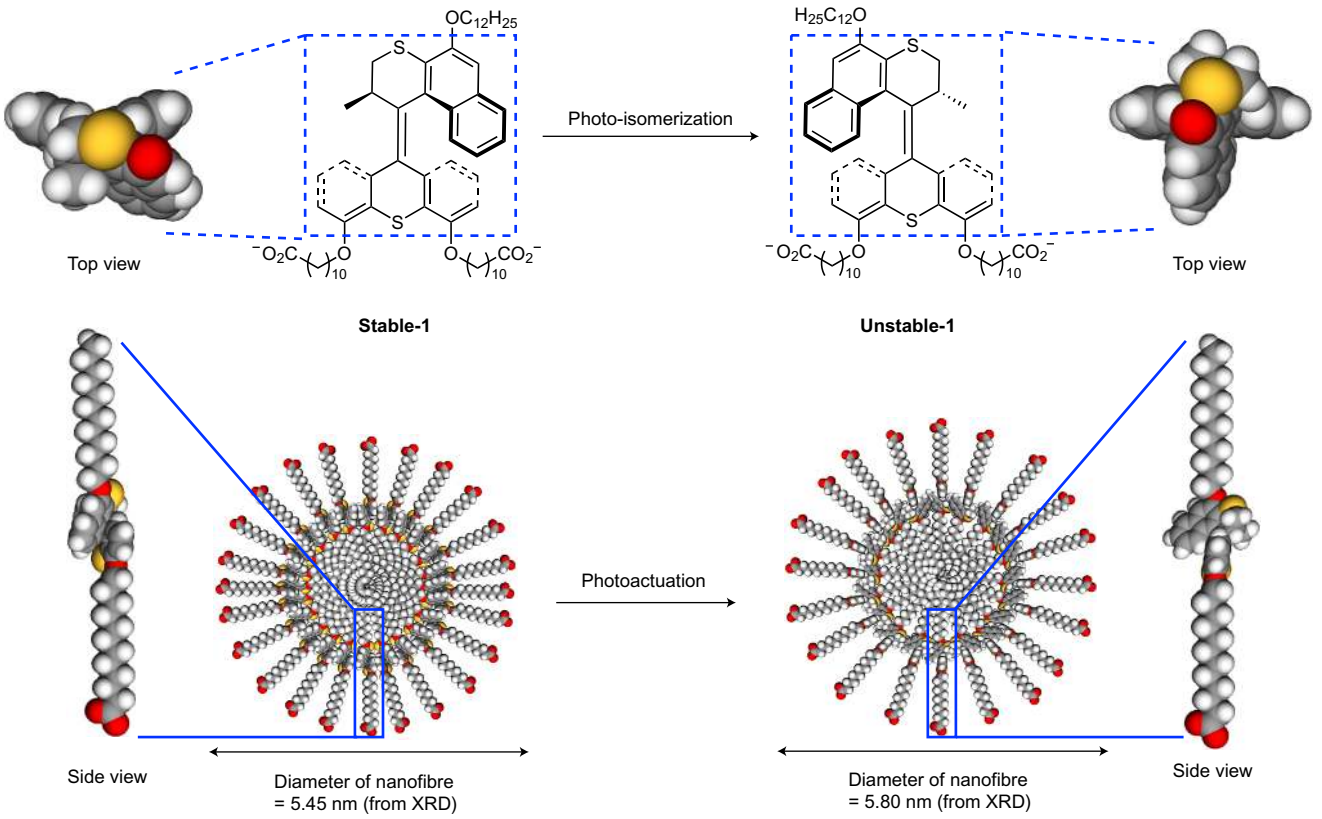

Figure 6 | Schematic illustration of the proposed mechanism of photoactuation. The structural change in the motor unit of **1** (shown with the space-filling model and chemical structure) upon photoisomerization (top) leads to an increase in the diameter of the nanofibres (bottom). Colour code of the space-filling model: grey, C; red, O; yellow, S; white, H.

holder designed specifically for this purpose (Fig. 5c). On exposure to the X-ray beam, the string gave a diffraction pattern (Fig. 5c, inset) that is essentially identical to that observed for a string on a sapphire (Fig. 3e,f). Following UV light irradiation for 20 s, the string bent by 25° towards the incident light source (Fig. 5d). As soon as the UV light was turned off, the bent string was exposed to the X-ray beam in the direction perpendicular to the UV light. As shown in Fig. 5d (inset), the *d* spacing of the diffraction from the (001) plane was clearly increased from 5.45 to 5.58 nm in the resulting SAXS pattern. The bent string was then irradiated again with UV light for 20 s (Fig. 5e). At this stage, the *d* spacing of the diffraction peak of the bent string was further increased to 5.60 nm (Fig. 5e, inset). Along with the change in the diffraction from the (001) plane, the intensities of the higher-order diffractions were reduced, suggesting partial disordering of assembled **1** inside the nanofibres. Following additional UV irradiation for 20 s (that is, 60 s irradiation in total), the bending angle of the string towards the light source increased to ~65° (Fig. 5f), and the corresponding SAXS pattern only showed diffraction from the (001) plane with a *d* spacing of 5.80 nm (Fig. 5f, inset). The increase in the *d* spacing due to the diffraction of the (001) plane indicates that this photoactuation process is accompanied by an increase in the diameter of the nanofibres. Furthermore, the pair of spot-like scatterings in a smaller-angle region ($q = 0.1–0.45$ nm^{-1}), which was initially observed in the horizontal direction (Fig. 5g), started to rotate in response to UV light, resulting in a tilt angle of 25° after 20 s irradiation, where the string bent by 25° (Fig. 5d). Similarly, when the string bent by 65° (Fig. 5f), the pair of spot-like scatterings rotated by 65° (Fig. 5h). The interesting consistency between the tilt angle of the scatterings and the bending angle of the string indicates that the macroscopic bending of the string is caused by orientational changes of the unidirectionally aligned nanofibre bundles.

Based on the results of *in situ* SAXS measurements, we propose a mechanism for the photoactuation. Following photochemical isomerization, motor **1** undergoes a structural change from the stable isomer to the unstable isomer, as indicated in Fig. 2. This change results in an increase of the excluded volume around the motor unit (Fig. 6), which in turn leads to a disturbance of the local packing arrangement in the motor amphiphile. Indeed, structural disordering was observed in the *in situ* SAXS measurements. At the same time, the diameters of the nanofibres expand, as represented by the gradual increase in the *d* spacing in the diffraction from the (001) plane of unidirectionally aligned nanofibre bundles. Assuming that the total volume of the string remains unchanged[36,37] throughout the photoactuation process, while the diameter of the individual nanofibres increases, the long axis of the string should contract. Considering the light absorbance by the motor unit and the thickness of the string (~300 μm), this contraction may occur only at the photoirradiated side of the string. As a consequence, the string bends towards the incident light source.

Conclusions

Our artificial supramolecular muscle system represents a unique photoactuator by which molecular motion can be amplified from the molecular level through various length scales to achieve a macroscopic mechanical function reminiscent of nature's ability to harness collective molecular motion. Hierarchical self-assembly of amphiphilic photoresponsive small-molecule rotary motors ($M_w < 1{,}000$ g mol^{-1}) in water, requiring a minimum of only 5 wt% of motors, provides unidirectionally aligned nanofibre bundles inside muscle-like strings that enable mechanical motion upon irradiation. Photo-controlled actuation is achieved both in aqueous solution and in air, including lifting weight, while localized actuation experiments indicate that precise control over the shape of

the strings can be achieved. *In situ* SAXS investigations suggest tight correlation from nanoscale motion of the motor to macroscopic photoactuation of the string. Distinctive features of this unique system include the finding that the non-covalent interactions of photoresponsive non-polymer-based molecules can sustain a muscle-like motion in water. For future bio-related applications, the highly dynamic nature of the materials (ready assembly–disassembly) and the non-invasive triggering with light might offer additional benefits. The demonstration of macroscopic mechanical motion based on a small molecule with an intrinsic rotary motor in a supramolecular assembly that functions as light-driven responsive material, both in water and air, provides an important step towards artificial mechanical materials and soft robotics.

Methods

Preparation of motor strings. Motor **1** (5.0 wt%) was mixed with 2 equiv. of NaOH in water. The obtained mixture was heated at 80 °C for 0.5 h and cooled to room temperature to afford a clear solution. When the obtained solution of motor **1** was manually drawn into an aqueous solution of $CaCl_2$ (150 mM) from a pipette, a noodle-like string with arbitrary length was formed. After removal of the solution of $CaCl_2$, the string was washed with deionized water (three times), and the resulting string was used directly for all POM and XRD experiments.

Actuation experiments in water and air. The aqueous solution of motor **1** prepared by the above method was manually drawn into an aqueous solution of $CaCl_2$ (150 mM) from a pipette. The obtained noodle-like string was kept in solution or pulled out of the water and suspended onto a sample holder for actuation experiments. Irradiation studies were performed with a Thorlab model M365FP1 high-power light-emitting diode (15.5 mW).

Data availability. Synthetic procedures, characterization data for all compounds, and extended experiments and discussions are provided in the Supplementary Information and are also available from the authors upon reasonable request.

Received 11 August 2017; accepted 2 October 2017; published online 4 December 2017

References

1. Vale, R. D. & Milligan, R. A. The way things move: looking under the hood of molecular motor proteins. *Science* **288,** 88–95 (2000).
2. Ueda, J., Schultz, J. A. & Asada, H. *Cellular Actuators: Modularity and Variability in Muscle-Inspired Actuation* (Butterworth-Heinemann, 2017).
3. Asaka, K. & Okuzaki, H. *Soft Actuators: Materials, Modeling, Applications, and Future Perspectives* (Springer, 2014).
4. Coskun, A., Banaszak, M., Astumian, R. D., Stoddart, J. F. & Grzybowski, B. A. Great expectations: can artificial molecular machines deliver on their promise? *Chem. Soc. Rev.* **41,** 19–30 (2012).
5. Balzani, V., Credi, A. & Venturi, M. *Molecular Devices and Machines: Concepts and Perspectives for the Nanoworld* (Wiley–VCH, 2008).
6. Morimoto, M. & Irie, M. A diarylethene cocrystal that converts light into mechanical work. *J. Am. Chem. Soc.* **132,** 14172–14178 (2010).
7. Kitagawa, D., Nishi, H. & Kobatake, S. Photoinduced twisting of a photochromic diarylethene crystal. *Angew. Chem. Int. Ed.* **52,** 9320–9322 (2013).
8. Ikegami, T., Kageyama, Y., Obara, K. & Takeda, S. Dissipative and autonomous square-wave self-oscillation of a macroscopic hybrid self-assembly under continuous light irradiation. *Angew. Chem. Int. Ed.* **55,** 8239–8243 (2016).
9. Kageyama, Y., Ikegami, T., Kurokome, Y. & Takeda, S. Mechanism of macroscopic motion of oleate helical assemblies: cooperative deprotonation of carboxyl groups triggered by photoisomerization of azobenzene derivatives. *Chem. Eur. J.* **22,** 8669–8675 (2016).
10. Feringa, B. L. *Molecular Switches* (Wiley–VCH, 2001).
11. Spencer, N. & Stoddart, J. F. A molecular shuttle. *J. Am. Chem. Soc.* **113,** 5131–5133 (1991).
12. Kay, E. R., Leigh, D. A. & Zerbetto, F. Synthetic molecular motors and mechanical machines. *Angew. Chem. Int. Ed.* **46,** 72–191 (2007).
13. Natansohn, A. & Rochon, P. Photoinduced motions in azo-containing polymers. *Chem. Rev.* **102,** 4139–4175 (2002).
14. Iwaso, K., Takashima, Y. & Harada, A. Fast response dry-type artificial molecular muscles with [c2]daisy chains. *Nat. Chem.* **8,** 626–633 (2016).
15. Li, Q. *et al.* Macroscopic contraction of a gel induced by the integrated motion of light-driven molecular motors. *Nat. Nanotech.* **10,** 161–165 (2015).
16. Foy, J. T. *et al.* Dual-light control of nanomachines that integrate motor and modulator subunits. *Nat. Nanotech.* **12,** 540–545 (2017).
17. Sidorenko, A., Krupenkin, T., Taylor, A., Fratzl, P. & Aizenberg, J. Reversible switching of hydrogel-actuated nanostructures into complex micropatterns. *Science* **315,** 487–490 (2007).
18. Ikeda, T., Mamiya, J. & Yu, Y. L. Photomechanics of liquid-crystalline elastomers and other polymers. *Angew. Chem. Int. Ed.* **46,** 506–528 (2007).
19. Camacho-Lopez, M., Finkelmann, H., Palffy-Muhoray, P. & Shelley, M. Fast liquid-crystal elastomer swims into the dark. *Nat. Mater.* **3,** 307–310 (2004).
20. Van Oosten, C. L., Bastiaansen, C. W. M. & Broer, D. J. Printed artificial cilia from liquid-crystal network actuators modularly driven by light. *Nat. Mater.* **8,** 677–682 (2009).
21. Iamsaard, S. *et al.* Conversion of light into macroscopic helical motion. *Nat. Chem.* **6,** 229–235 (2014).
22. Lv, J. A. *et al.* Photocontrol of fluid slugs in liquid crystal polymer microactuators. *Nature* **537,** 179–184 (2016).
23. Jimenez, M. C., Dietrich-Buchecker, C. & Sauvage, J. P. Towards synthetic molecular muscles: contraction and stretching of a linear rotaxane dimer. *Angew. Chem. Int. Ed.* **39,** 3284–3287 (2000).
24. Jimenez-Molero, M. C., Dietrich-Buchecker, C. & Sauvage, J. P. Towards artificial muscles at the nanometric level. *Chem. Commun.* 1613–1616 (2003).
25. Lehn, J. M. Perspectives in supramolecular chemistry—from molecular recognition towards molecular information-processing and self-organization. *Angew. Chem. Int. Ed.* **29,** 1304–1319 (1990).
26. Aida, T., Meijer, E. W. & Stupp, S. I. Functional supramolecular polymers. *Science* **335,** 813–817 (2012).
27. Xue, B. *et al.* Electrically controllable actuators based on supramolecular peptide hydrogels. *Adv. Funct. Mater.* **26,** 9053–9062 (2016).
28. Bruns, C. J. & Stoddart, J. F. Rotaxane-based molecular muscles. *Acc. Chem. Res.* **47,** 2186–2199 (2014).
29. Collin, J. P., Dietrich-Buchecker, C., Gavina, P., Jimenez-Molero, M. C. & Sauvage, J. P. Shuttles and muscles: linear molecular machines based on transition metals. *Acc. Chem. Res.* **34,** 477–487 (2001).
30. Goujon, A. *et al.* Hierarchical self-assembly of supramolecular muscle-like fibers. *Angew. Chem. Int. Ed.* **55,** 703–707 (2016).
31. Goujon, A. *et al.* Controlled sol–gel transitions by actuating molecular machine based supramolecular polymers. *J. Am. Chem. Soc.* **139,** 4923–4928 (2017).
32. Krieg, E., Bastings, M. M. C., Besenius, P. & Rybtchinski, B. Supramolecular polymers in aqueous media. *Chem. Rev.* **116,** 2414–2477 (2016).
33. Webber, M. J., Appel, E. A., Meijer, E. W. & Langer, R. Supramolecular biomaterials. *Nat. Mater.* **15,** 13–26 (2016).
34. Zhang, S. M. *et al.* A self-assembly pathway to aligned monodomain gels. *Nat. Mater.* **9,** 594–601 (2010).
35. Koumura, N., Geertsema, E. M., van Gelder, M. B., Meetsma, A. & Feringa, B. L. Second generation light-driven molecular motors. Unidirectional rotation controlled by a single stereogenic center with near-perfect photoequilibria and acceleration of the speed of rotation by structural modification. *J. Am. Chem. Soc.* **124,** 5037–5051 (2002).
36. Goodby, J. W. *et al. Handbook of Liquid Crystals* 2nd edn (Wiley-VCH, 2014).
37. Kim, Y. S. *et al.* Thermoresponsive actuation enabled by permittivity switching in an electrostatically anisotropic hydrogel. *Nat. Mater.* **14,** 1002–1007 (2015).

Acknowledgements

This work was supported financially by the Netherlands Organization for Scientific Research (NWO-CW), the European Research Council (ERC, advanced grant no. 694345 to B.L.F.), the Ministry of Education, Culture and Science (Gravitation Program no. 024.001.035) and a Grant-in-Aid for Scientific Research on Innovative Areas 'π-Figuration' (nos. 26102008 and 15K21721) of The Ministry of Education, Culture, Sports, Science and Technology (MEXT), Japan. The synchrotron XRD experiments were performed at BL45XU in SPring-8 with the approval of the RIKEN SPring-8 Center (proposal no. 20160027).

Author contributions

B.L.F., F.K.-C.L. and J.C. conceived the research. J.C. and F.K.-C.L. carried out the synthesis of **1**. J.C. characterized the motion of the molecular motor. M.C.A.S. performed the cryo-TEM. F.K.-C.L. prepared the string and carried out POM and SEM analysis. F.K.-C.L. and T.K. performed all XRD measurements and structural analysis. J.C. and F.K.-C.L. carried out the actuation experiments. J.C. and E.v.d.G. analysed and calculated the mechanical work. J.C., F.K.-C.L., T.K., T.F. and B.L.F. co-wrote the paper. All authors discussed the results and commented on the manuscript.

Additional information

Supplementary information and chemical compound information are available in the online version of the paper. Reprints and permissions information is available online at www.nature.com/reprints. Publisher's note: Springer Nature remains neutral with regard to jurisdictional claims in published maps and institutional affiliations. Correspondence and requests for materials should be addressed to B.L.F.

Competing financial interests

The authors declare no competing financial interests.